Annual Methodological Archive Research Review
http://amresearchreview.com/index.php/Journal/about
Volume 3, Issue 10 (2025)

Online ISSN 3007-3197
Print ISSN 3007-3189

http://amresearchreview.com/index.php/Journal/about

A Review On Localized Surface Plasmon Resonance (LSPR) Based Optical Sensing

Muhammad Abdur Rehman
The Superior University, Lahore
Email: badshahjee367@gmail.com

Zeeshan Mahmood
The Superior University, Lahore
Email: badshahjee367@gmail.com

ABSTRACT

In nanoplasmonics, Localized Surface Plasmon Resonance (LSPR) is a crucial phenomenon that provides great sensitivity for optical sensing applications. It originates from the collective oscillation of light-excited conduction electrons in metallic nanoparticles. Peak position, intensity, and sensitivity to surrounding media are among the LSPR characteristics that are strongly influenced by the form of these nanoparticles. This review concentrates on LSPR-based optical sensors, highlighting the ways in which various nanoparticle shapes, such as stars, cubes, triangles, spheres, rods, and other anisotropic geometries, affect sensing capabilities. We evaluate how form affects detection limits, resonance tunability, and electric field enhancement, as demonstrated by both numerical simulations and experimental data. The impact of shape-induced plasmonic modes on sensing applications specifically, chemical detection and biosensing is examined.

Key Words: LSPR, Optical Sensor, detection limits, Biosensing

Introduction:

Nanotechnology has been studied for more than a century. Nanoparticles (NPs) constitute a generic group of materials that encompasses particulate material with a diameter smaller than 100 nanometers (Ockwig et al., 2010). Nanometer-sized particles have attracted significant interest over the last few years because of the tunability of electronic and optical properties with molecular dimensions. Localized surface plasmon resonance (LSPR) is a thoroughly investigated nanoscale phenomenon that has garnered significant attention in recent times (K. M. Mayer & Hafner, 2011). The most interesting feature is the localized surface plasmon resonances of Au nanocrystals (LSPRs). The free-electron collective oscillations confined to the nanoscale are associated with LSPRs, which are electromagnetic modes (Chen et al., 2013).

Annual Methodological Archive Research Review
http://amresearchreview.com/index.php/Journal/about
Volume 3, Issue 10 (2025)

Online ISSN 3007-3197
Print ISSN 3007-3189

http://amresearchreview.com/index.php/Journal/about

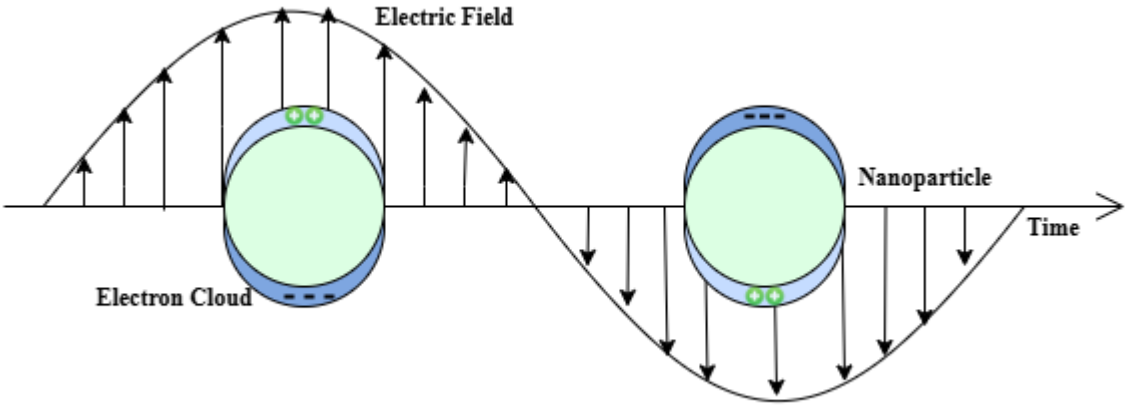
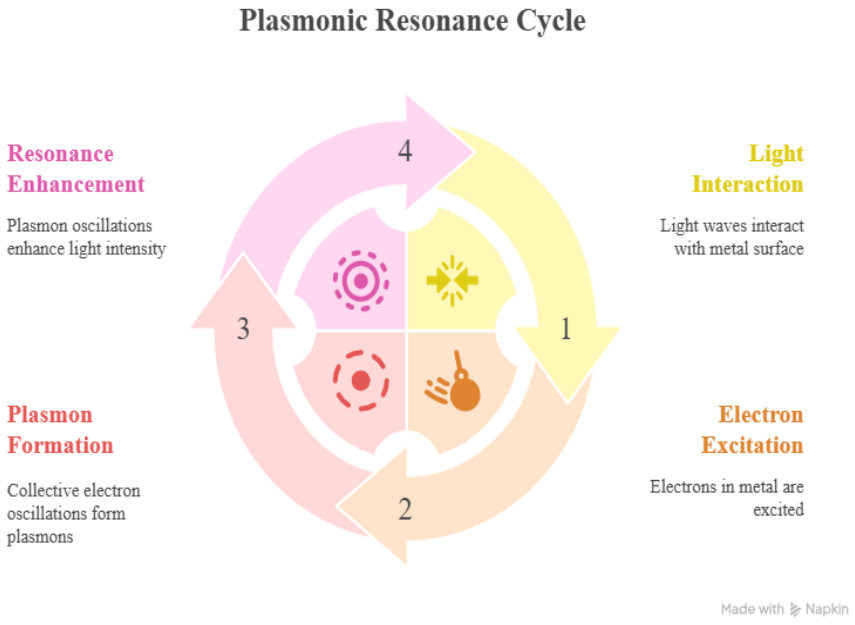


Figure 1: Localized surface plasmon resonance (LSPR) is observed where the free conduction electrons in the metal nanoparticle are driven into oscillation due to strong coupling with incident light.

Transverse surface Plasmon resonance absorption is associated with the wavelengths between 510 nm and 530 nm, where the free electrons along the shorter axis of the rod come into resonance with light. The vibrations down the long axis arise from the scattering of incident light by the rod, which can thus range from visible to near-infrared and is called longitudinal LSPR (Meng et al., 2019).



Annual Methodological Archive Research Review
http://amresearchreview.com/index.php/Journal/about
Volume 3, Issue 10 (2025)

Online ISSN 3007-3197
Print ISSN 3007-3189
http://amresearchreview.com/index.php/Journal/about

Figure 2: Schematic Diagram of Plasmon cycle

The capabilities of noble metal nanoparticle (NP) localized surface plasmon resonance (LSPR) in connection with optical fibers for the production of LSPR optical fiber sensors has become a field of great research (Jin et al., 2003). The localized electromagnetic field that surrounds the metal surface reacts highly to any refractive index changes in the environment. Changes in the LSPR properties of metals can then be exploited to track environmental variations in the interaction of media with metal. Depending on whether the biosensor is colloidal or chip-based, LSPR biosensing can be divided into two basic classes. Colloidal-based LSPR sensing systems have also been developed to detect environmental contaminants, toxins, and biological agents(Leosson & Agnarsson, 2012).

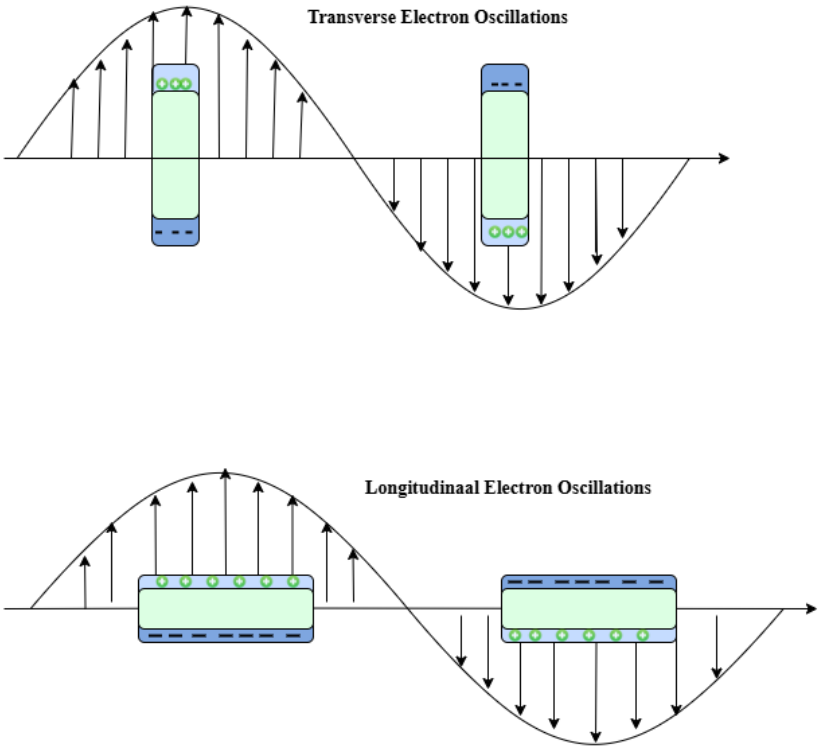


Figure 3: Longitudinal and transverse plasmon bands corresponding to the electron oscillations. (Made by draw.io)

Mie's theory was used to study the light scattering and absorption due to spherical nanoparticles by solving Maxwell's equations. Mie's theory explains how electromagnetic waves interact with MNPs at surface boundaries(Paz et al., 2012). The complex permittivity of the MNPs as calculated from Drude's theory, is also a significant parametric function for the calculation of the light scattering and absorption due to the spherical nanoparticle. The limitation on the nanostructure's outside causes

Annual Methodological Archive Research Review
http://amresearchreview.com/index.php/Journal/about
Volume 3, Issue 10 (2025)

Online ISSN 3007-3197
Print ISSN 3007-3189
http://amresearchreview.com/index.php/Journal/about

a refractive file change, resulting in a change in the extinction wavelength max. The accompanying condition determines the change in max.

$$\Delta\lambda max \cong m\Delta n\,[1-((-2d)/Id)] \qquad (1)$$

The sensitivity factor is denoted by the letter 'm'. The refractive index change is n, and the effective adsorbate layer thickness is d. The EM field decay length is denoted by the letter 'I'(Nanoph-2016-0101-1.Pdf, n.d.) Mie theoretically described this classic effect in 1908 by solving Maxwell's equations for a plane wave impacting on a metal sphere surrounded by a dielectric medium, given the metal's dielectric function. In terms of a multipole expansion, Mie theory provides an exact analytical solution for nanoparticle LSPR(Nehl & Hafner, 2008).

Localized Surface Plasmon Resonance

Localized Surface Plasmons (LSPs) are oscillations generated by the free electrons in metallic nanoparticles when subjected to electromagnetic waves with wavelengths greater than the NP dimension. Resonance occurs when the surface plasmon (SP) wave vector corresponds to the incident light wave vector. The SP wave vector can be calculated using Maxwell's theory. Using the appropriate boundary conditions, the wave vectors of the surface plasmon are:

$$K_{sp} = \frac{\omega}{c}\sqrt{\frac{\varepsilon_m \varepsilon_d}{\varepsilon_m + \varepsilon_d}}$$

and the wave vector of incident light is:

$$K_x = \frac{\omega}{c}\sqrt{\varepsilon_p}\sin\theta_i$$

where εp, εm, and εd indicate the dielectric constant of the prism, metal, and dielectric, respectively, while θi indicates the incident angle. Resonance can be achieved by changing the incidence angle and it can be predicted mathematically by the following equation:

$$\theta_{res} = \sin^{-1}\left(\frac{1}{\sqrt{\varepsilon_p}}\sqrt{\frac{\varepsilon_m \varepsilon_d}{\varepsilon_m + \varepsilon_d}}\right)$$

In some literature, the resonance angle (θres) is referred to as the SPR angle. The refractive index material np allows the incident light propagation constant k to couple with the SP wave vector at the intersection point, indicating resonance conditions.

Plasmonic Material and LSPR Performance

LSPR can theoretically be achieved in any metal, semiconductor, or compound, provided the Froehlich condition is satisfied and Re[$\in$**1**]< 0 due to free transporters. Due to the LSPR top at a visible area, Cu, Au, and Ag are the most commonly used LSPR metals. Al also has Plasmon reverberation in the bright area, where a few natural particles keep the light. The destinations of Na, Li, and Ga are all viable options. Plasmon illustration of reverberation in the UV-Visible spectrum, as well as the Frohlich rule However, these basic materials are easily oxidized and extremely

Annual Methodological Archive Research Review
http://amresearchreview.com/index.php/Journal/about
Volume 3, Issue 10 (2025)

Online ISSN 3007-3197
Print ISSN 3007-3189
http://amresearchreview.com/index.php/Journal/about

sensitive to the environment, limiting their application as biosensor stages. Materials with a real negative component (Re) [∈_1] and a small certain imaginary part (Im) [∈_1] work on the dielectric in general to meet the Frohlich model(Maier et al., 2007). To make a metallic Nano sphere, For (Re)[∈_1]≈-2, which is attained at frequencies, the Fröhlich in vacuum model is achieved. Cu has a wavelength of 300 nanometers, Ag has a wavelength of 350 nanometers, and Au has a wavelength of 490 nanometers (Hein & Maier, 2007).

The LSPR and Size of Nanoparticle

The light-NP interaction is influenced by the size of the metallic nanostructure. The dipole contribution to the LSPR spectra is increased by shrinking metallic NPs. Higher order modes (e.g., quadrupoles) can considerably contribute to the particle extinction cross section by expanding the radius of NPs. The size of scattering and absorption cross sections is true. The absorption cross section of a spherical nanoparticle is proportional to the third power of the NP radius in a quasi-static approximation, while the scattering cross section is proportional to the sixth power of the particle radius(Wriedt, 2008). As a result, the light-NP interaction is mostly determined by scattering for larger metallic nanostructures (average sizes greater than 50 nm). The scattering cross sections of metallic NPs grow as their size increases.

Mie derived an expression for particle polarizability and, as a result, for its extinction cross-section by solving Maxwell's equations for an electromagnetic wave interacting with a sphere considerably smaller than the light wavelength (2r is very, very small than the wavelength where r is the sphere radius)(Wriedt, 2008). The polarizability is measured in degrees of polarizability.

$$\boldsymbol{\alpha = 4\pi r^3 \frac{\epsilon_1 - \epsilon_2}{\epsilon_1 + 2\,\epsilon_2}}$$

When the real component of ϵ_1 equals $-2\epsilon_2$, the enhancement decreases as $\epsilon_1+2\epsilon_2$ approaches zero. The Fröhlich condition describes this link (Maier et al., 2007).

The termination cross-segment of a nanoparticle can be determined by its assimilation (δabs) and dispersion (δsca) cross-segments, which depend on the polarizability of the molecule.

$$\boldsymbol{\delta_{sca} = \frac{K^4}{6\pi}|\alpha|^2}$$

$$\boldsymbol{\delta_{abs} = KIm|\alpha|}$$

The absorption and scattering cross sections depend on the particle radius in various ways; hence, particle size has a significant impact on its LSPR (Grasseschia, n.d.).

Annual Methodological Archive Research Review
http://amresearchreview.com/index.php/Journal/about
Volume 3, Issue 10 (2025)

Online ISSN 3007-3197
Print ISSN 3007-3189

http://amresearchreview.com/index.php/Journal/about

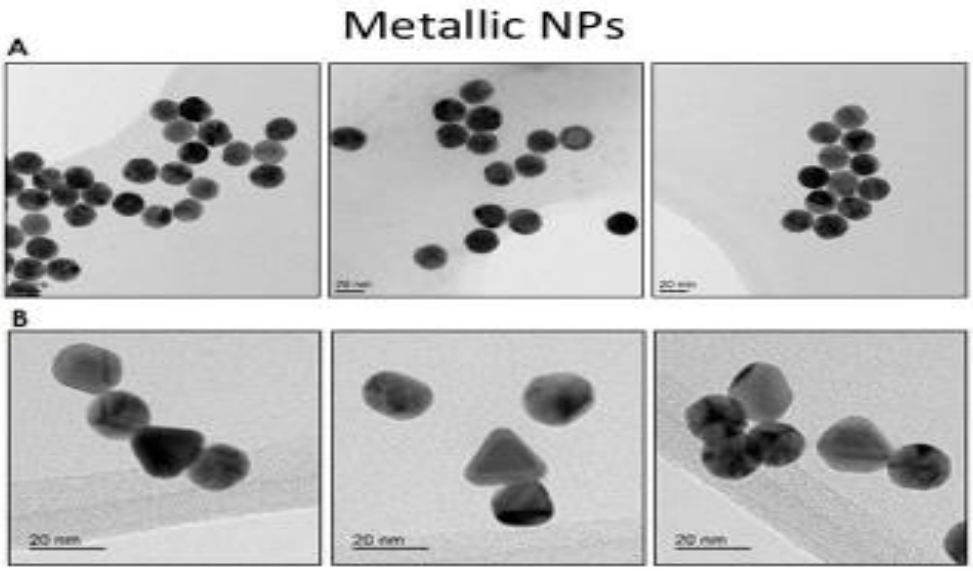


Figure 4: Dependence of LSPR wavelength position on the shape and size of nanoparticles (DOI:10.15407/spqeo24.03.304**)**

The LSPR and Nanoparticle Shape

Modifying the metallic NP shape can cause changes in LSPR characteristics, allowing the Plasmon peak to be rendered in a variety of spectral ranges. Compared to spheroids, NPs with sharper points are expected to exhibit LSPR at longer wavelengths(Moe & Chen, 2008). Nano triangles have a redder plasmonic peak than cubic nanostructures because their points are sharper. AuNPs were manufactured in a variety of shapes, including nanospheres, nanorods, nanocubes, nanobranches, and nanobipyramids, and shape-dependent LSPR was investigated in the visible to near-infrared range (A. R. Bijanzadeh, 2012).

Enhancement of the Field

Localized surface plasmon resonance is the collective oscillation of electrons within noble metal nanostructures allows for resonant excitation of light at a specific wavelength. At the resonant wavelength, metal nanostructures exhibit enhanced local electric fields (E fields) on their surfaces (Farooq, Gomez Malagon, et al., 2019). These enhanced E fields account for the majority of the surface-enhanced Raman scattering (SERS) intensity. The electric field inside and outside of a metallic nanoparticle can be amplified when the Fröhlich condition is met. For example, the inside (E) and outside (E) distributions of the local field of a metallic nanosphere can be evaluated as (Hyun & Han, 2012):

$$\mathbf{E_{in}} = \frac{\mathbf{3}\ \epsilon_2}{\epsilon_1 + \mathbf{2}\ \epsilon_2} \times \mathbf{E_o}$$

Annual Methodological Archive Research Review
http://amresearchreview.com/index.php/Journal/about
Volume 3, Issue 10 (2025)

Online ISSN 3007-3197
Print ISSN 3007-3189
http://amresearchreview.com/index.php/Journal/about

$$\mathbf{E_{out}} = \mathbf{E_o} + \frac{\mathbf{3n(n.p) - p}}{\epsilon_1 + \mathbf{2}\ \epsilon_2} \times \mathbf{E_O}\frac{\mathbf{1}}{\mathbf{r^3}}$$

where n and p are the oscillating dipole moment and a unit vector normal to the surface, respectively. The E-field enhancement (EF) of the LSPR around the nanoparticle is defined as follows:

$$\mathbf{EF_F} = \frac{|\mathbf{E_{max}}|}{|\mathbf{E_o}|}$$

Where E° denotes the incident field and EF_F denotes the maximal electric field around a nanoparticle's surface. At their plasmonic resonances, non-spherical forms have larger field enhancements.

Graphene

Graphene, a two-dimensional material composed of a single layer of carbon atoms arranged in a honeycomb lattice, has been identified as a promising material for a wide range of applications, including transparent electronics, gate modulators, photo catalysts, and others(Fang et al., 2014). When graphene is sliced into nanostructures, surface plasmons can be stimulated in specific locations. This generates plasmonic standing waves at the resonant frequencies, which eliminates the need for additional wave vector matching techniques(Ju et al., 2011). .

The first application of graphene LSPR was in monolayer graphene microribbons. Shortly after, LSPR was discovered in graphene microdisks, which had a similar otherworldly reach. Similarly, stacking multiple graphene circles or strips separated by thin dielectrics was shown to provide an additional method for obtaining phantom tenability via interlayer Coulomb interactions (Yan et al., 2012). The structures displayed were suitable for use as filters and polarizers. Later, an ATHz photodetector using LSPR was demonstrated on a bilayer graphene microribbon. Furthermore, an array of micro holes (or antidotes) has been shown to produce electrically tunable LSPR in the THz region, with multiple absorption bands observed. Nanostructures are typically required to operate in the mid-infrared spectrum, and one such example is LSPR in nanoribbons (Rodrigo et al., 2015). .

The current barrier to widespread use of graphene LSPR devices is the high cost of creating graphene nanostructures through electron beam lithography, which limits scalability (Wang et al., 2016). Self-assembly of block copolymers was used as a more scalable method of creating a mask for etching graphene nanodisks. Spin coating was used to apply polystyrene-b-polydimethylsiloxane (PS-PDMS) to graphene. Nanoimprinting lithography was also utilized to create scalable arrays of nano-holes (López-Muñoz et al., 2017).

Plasmonic Sensing Principles

Shift in Plasmon Energy

Changes in the NP local environment have a significant impact on LSPR. The polarizability of NP is determined by ϵ_2; as the RI of the surrounding medium changes, so does the Fröhlich condition and the Plasmon peak (Verellen et al., 2011). The refractive index sensitivity of an LSPR sensor, denoted as, is used to evaluate its

Annual Methodological Archive Research Review
http://amresearchreview.com/index.php/Journal/about
Volume 3, Issue 10 (2025)

Online ISSN 3007-3197
Print ISSN 3007-3189
http://amresearchreview.com/index.php/Journal/about

performance (K. M. Mayer, 2010).

$$\mathbf{S_n = \frac{\Delta\lambda_{LSPR}}{\Delta\mu_2}}$$

LSPR sensors detect nanoparticles with sharp ends, including nanosats, nanowires, nanorods, and nanocrescents. They have a high affectability and can introduce low FoM esteems due to their diverse performance. Altering mathematical boundaries can improve LSPR affectability.

The LSPR phantom data transport capacity may limit the detection of simple alterations in the reverberation peak. As a result, significant amounts of money are saved. The Figure of Merit (FoM) for the plasmonic sensor is as follows:

$$\mathrm{FoM} = \frac{\mu_2}{\mathrm{FWHM}}$$

Table 1: Figures of merit for nanostructures on LSPR platforms

Nano Structure	Types	$\mathbf{S_n(nmRIU^{-1})}$	FoM	$\mathbf{S_n \times FoM\ (nmRIU^{-2})}$	References
Au Shell	Single	381	5.4	2057.4	(Farooq, Rativa, et al., 2019)
Au pyramid	Single	221	2.2	486.2	(S. Lee & Heo, 2009)
Au rattle	Single	199	3.8	756.2	(Khalavka et al., 2009)
Au rods	Ensemble	170	1.3	221.0	(J. D. Mayer et al., 2008)
Au Star	Single	238	1.9	452.2	(Nehl et al., 2006)

The FWHM of the LSPR peak represents the full width half maximum. A plasmonic sensor must meet both high sensitivity and a crisp LSPR spectrum. Complex plasmonic devices are being investigated for sensing applications even though the LSPR peak is broad (Farooq, Rativa, et al., 2019).

Annual Methodological Archive Research Review
http://amresearchreview.com/index.php/Journal/about
Volume 3, Issue 10 (2025)

Online ISSN 3007-3197
Print ISSN 3007-3189
http://amresearchreview.com/index.php/Journal/about

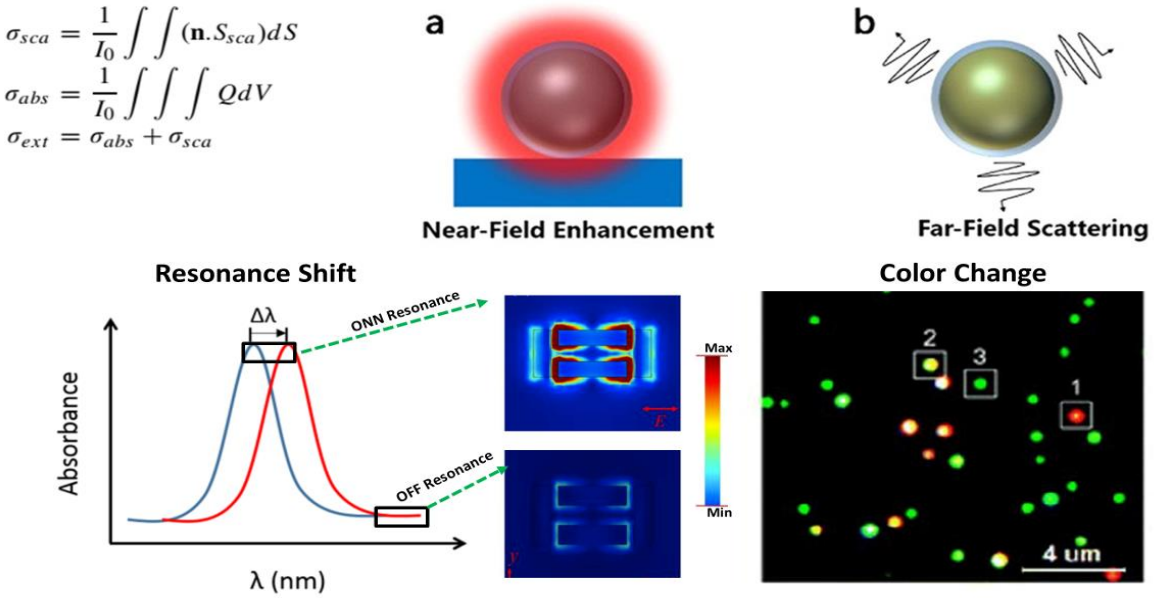


Figure 5: The four contributions to the SERS effect are depicted in this diagram. The electromagnetic mechanism, the resonant chemical mechanism, the Effect Resonant Raman mechanism, and the non-resonant chemical mechanism are all examples of mechanisms. Adopted from (Grasseschia, n.d.).

Plasmon Resonances and Energy Transfer

Plasmon resonance energy transfer is the coherent transfer of energy from surface plasmons to nearby exciton nanosystems, like dye molecules or semiconductor quantum dots, through dipole-dipole coupling (Zhang et al., 2018). A non-radiative plasmon decay pathway, the plasmon resonance energy transfer can also serve as an accessible channel for the extraction of plasmon-harvested energy. Additionally, the dissipation pathways of surface plasmon resonances include scattering (radiative channel) and hot electron relaxation (non-radiative channel).

Annual Methodological Archive Research Review
http://amresearchreview.com/index.php/Journal/about
Volume 3, Issue 10 (2025)

Online ISSN 3007-3197
Print ISSN 3007-3189
http://amresearchreview.com/index.php/Journal/about

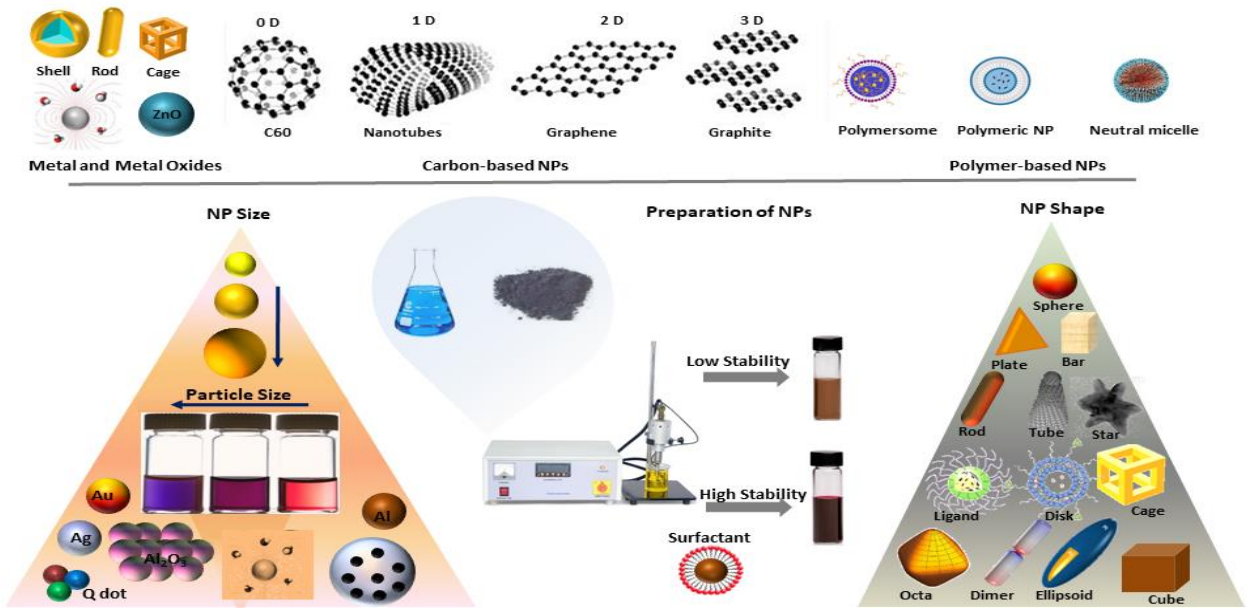


Figure 6: LSPR excitation and potential pathways for energy transfer for different uses. (a) A strong local field produced by LSPR causes scattering and more light trapping. (b) Plasmon-induced energy transfer (PIRET), which is the direct transfer of charges from the valence band (VB) to the conduction band (CB), leading to optical absorption. (c) By producing local heat, LSPR excitation can dephase. (d) The heat generated by dephasing allows for plasmon–phonon interaction Farooq, Sajid, et al, Advances in Colloid and Interface Science (2025): 103495.

The energy of excited plasmons can be used in many different ways due to radiative and non-radiative decays (dos Santos & Grasseschi, 2020). Energy transfer processes lead to fluorescence amplification when fluorescent species (molecules or semiconductors) are introduced close to plasmonic nanoparticles. Photon emission from the Plasmon's radiative decay is the main source of the energy transfer (Govorov et al., 2007). Antenna effect brought on by this decay raises incident radiation intensity close to the surface, where more excited states can form.

The creation of excited states is influenced by the distance between the molecule and the surface of the nanoparticle. The intensification effect in the formation of excited states in a system can be measured by a molecule's fluorescence intensity; the greater this effect, the more intense the fluorescence. Scaiano et al. used an AFM tip coated with 80 nm AuNP to measure the fluorescence intensity of a molecule on a fixed substrate as a function of distance (R). In the primary area, where the fluorophore was situated less than 2 nm from the surface of the nanoparticle, there was a reported extinguishment of fluorescence with a reduction (Grasseschia, n.d.). Somewhere far away, among AuNP and the fluorophore on the surface of the nanoparticle, there was a reduction that caused the fluorescence to extinguish due to electron movements. The energy differential between the two halves of the nanoparticle is what drives these exchanges. The Fermi level, the atom, and the degree of particle orbital interaction involving the surface of the molecule (Cushing et al., 2015).

Annual Methodological Archive Research Review
http://amresearchreview.com/index.php/Journal/about
Volume 3, Issue 10 (2025)

Online ISSN 3007-3197
Print ISSN 3007-3189
http://amresearchreview.com/index.php/Journal/about

In the second region, where the distance between the fluorophore and the plasmonic surface ranges from 3 to 30 nm, the fluorophore is stimulated by either the Plasmon's electric field or photons released by Plasmon decay. To maximize FRET, the emission spectra of the fluorophore and the LSPR band must overlap. There have been reports of a more noticeable emission boost for R between 40 and 60 nm. The optimal R, which combines absorption and emission enhancement, should be between 3 and 15 nm (Li et al., 2016).

References

R. Bijanzadeh. (2012). A study of the surface plasmon absorption band for nanoparticles. International Journal of Physical Sciences, 7(13). https://doi.org/10.5897/ijps11.893

Alarcon, E. I., Bueno-Alejo, C. J., Noel, C. W., Stamplecoskie, K. G., Pacioni, N. L., Poblete, Batista, E. A., Santos, D. R. D., Andrade, G. F. S., Sant'Ana, A. C., BroIo, A. G., & Temperin, M. L. A. (2009). Using polycarbonate membranes as templates for the preparation of au nanostructures for surface-enhanced raman scattering. Journal of Nanoscience and Nanotechnology, 9(5), 3233–3238. https://doi.org/10.1166/jnn.2009.209

Chen, H., Shao, L., Li, Q., & Wang, J. (2013). Gold nanorods and their plasmonic properties. Chemical Society Reviews, 42(7), 2679–2724. https://doi.org/10.1039/c2cs35367a

Cushing, S. K., Li, J., Bright, J., Yost, B. T., Zheng, P., Bristow, A. D., & Wu, N. (2015). Controlling Plasmon-Induced Resonance Energy Transfer and Hot Electron Injection Processes in Metal@TiO2 Core-Shell Nanoparticles. Journal of Physical Chemistry C, 119(28), 16239–16244. https://doi.org/10.1021/acs.jpcc.5b03955

dos Santos, D. P., & Grasseschi, D. (2020). Plasmonic nanomaterials: Part II. Surface coordination chemistry and its application to sensors and catalysts. Quimica Nova, 43(10), 1482–1499. https://doi.org/10.21577/0100-4042.20170629

Fang, Z., Thongrattanasiri, S., Schlather, A., Liu, Z., Ma, L., Wang, Y., Ajayan, P. M., Nordlander, P., Halas, N. J., & García De Abajo, F. J. (2013). Gated tunability and hybridization of localized plasmons in nanostructured graphene. ACS Nano, 7(3), 2388–2395. https://doi.org/10.1021/nn3055835

Fang, Z., Wang, Y., Schlather, A. E., Liu, Z., Ajayan, P. M., García De Abajo, F. J., Nordlander, P., Zhu, X., & Halas, N. J. (2014). Active tunable 002.absorption enhancement with graphene nanodisk arrays. Nano Letters, 14(1), 299–304. https://doi.org/10.1021/nl404042h

Farooq, S., Gomez Malagon, L. A., De Araujo, R. E., & Rativa, D. (2019). Spherical Plasmonic Structures for Solar Absorption. 2018 SBFoton International Optics and Photonics Conference, SBFoton IOPC 2018, April 2020, 1–4. https://doi.org/10.1109/SBFoton-IOPC.2018.8610899

Farooq, S., Rativa, D., & de Araujo, R. E. (2019). Optimizing the Sensing Performance of SiO2-Au Nanoshells. Plasmonics, 14(6), 1519–1526. https://doi.org/10.1007/s11468-019-00947-4

Online ISSN 3007-3197
Print ISSN 3007-3189
http://amresearchreview.com/index.php/Journal/about

Foerster, S., Linnainmaa, J. T., Melzer, B. T., & Previtero, A. (2017). Retail Financial Advice: Does One Size Fit All? Journal of Finance, 72(4), 1441–1482. https://doi.org/10.1111/jofi.12514

Giannini, V., Fernández-Domínguez, A. I., Heck, S. C., & Maier, S. A. (2011). Plasmonic nanoantennas: Fundamentals and their use in controlling the radiative properties of nanoemitters. Chemical Reviews, 111(6), 3888–3912. https://doi.org/10.1021/cr1002672

Mahmood, H.Z., Farooq, S., Lins, E.C., 2019. Optimizing the Plasmonic Sensing of Silica Coated Au/Ag Nanoshells. Int J Sci Eng InvestigIJSEI 8, 140–145.

Hein, M., & Maier, M. (2007). Manifold denoising as preprocessing for finding natural representations of data. Proceedings of the National Conference on Artificial Intelligence, 2(Taubin 1995), 1646–1649.

Computational Linguistics, ACL 2016 - Long Papers, 2, 994–1003. https://doi.org/10.18653/v1/p16-1094

Lombardi, J. R., & Birke, R. L. (2014). Theory of surface-enhanced raman scattering in semiconductors. Journal of Physical Chemistry C, 118(20), 11120–11130. https://doi.org/10.1021/jp5020675

MAHMOOD, H.Z., 2019. A study of metallic and polymeric nanostructure-solution based platforms for optical and chemical arbovirus biosensing.

Maier, M., Hein, M., & Von Luxburg, U. (2007). Cluster identification in nearest-neighbor graphs. Lecture Notes in Computer Science (Including Subseries Lecture Notes in Artificial Intelligence and Lecture Notes in Bioinformatics), 4754 LNAI(May), 196–210. https://doi.org/10.1007/978-3-540-75225-7_18

Farooq, S., Mahmood, H.Z., Rativa, D., Bouchonneau, N., Lins, E., Fontana, J., de Araujo, R.E., 2018. Optimizing gold nanorods dimer structure for sensing platform, in: 2018 SBFoton International Optics and Photonics Conference (SBFoton IOPC). IEEE, pp. 1–4.

Mayer, K. M., & Hafner, J. H. (2011). Localized surface plasmon resonance sensors. Chemical Reviews, 111(6), 3828–3857. https://doi.org/10.1021/cr100313v

nanoph-2016-0101-1.pdf. (n.d.).

Nehl, C. L., & Hafner, J. H. (2008). Shape-dependent plasmon resonances of gold nanoparticles. Journal of Materials Chemistry, 18(21), 2415–2419. https://doi.org/10.1039/b714950f

Nehl, C. L., Liao, H., & Hafner, J. H. (2006). Optical properties of star-shaped gold nanoparticles. Nano Letters, 6(4), 683–688. https://doi.org/10.1021/nl052409y

Ockwig, N. W., Nenoff, T. M., Separation, H., Rev, C., Chem, E., Laurent, S., Forge, D., Port, M., Roch, A., Robic, C., Elst, L. Vander, & Muller, R. N. (2010). Additions and corrections. 110(4), 2573–2574.

Shad, N.A., Jameel, A., Sajid, M.M., Afzal, A.M., Javed, Y., Ullah, A., Asghar, A., Mehmood, Z., Kiran, I., Munawar, A., Qayyum, M.A., Sarwar, M., 2022. Fabrication of Spike-Like Spherical Iron Manganite Nanoparticles for the Augmented Photocatalytic Degradation of Methylene Blue Dye. J. Electron. Mater. 51, 900–909. https://doi.org/10.1007/s11664-021-09371-z

Farooq, S., da Silva Correia, T.T., Yoshimura, T.M., de Toledo Pereira, S., Ribeiro, M.S., de Araujo, R.E. (2019). Methylene Blue-Mediated Photoinactivation

Online ISSN 3007-3197
Print ISSN 3007-3189

of Staphylococcus aureus Assisted by Gold Nanoshells. In: Costa-Felix, R., Machado, J., Alvarenga, A. (eds) XXVI Brazilian Congress on Biomedical Engineering. IFMBE Proceedings, vol 70/2. Springer, Singapore. https://doi.org/10.1007/978-981-13-2517-5_130